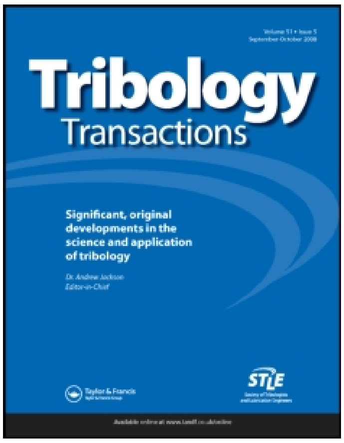

Tribology Transactions
Publication details, including instructions for authors and subscription information:
http://www.informaworld.com/smpp/title~content=t713669620

The Effect of Novel Surface Textures on Tappet Shims on Valvetrain Friction and Wear

Arup Gangopadhyay[a]; Douglas G. McWatt[a]
[a] Research and Innovation Center, Ford Motor Company, Dearborn, MI

First published on: 01 March 2008

To cite this Article Gangopadhyay, Arup and McWatt, Douglas G.(2008) 'The Effect of Novel Surface Textures on Tappet Shims on Valvetrain Friction and Wear', Tribology Transactions, 51: 2, 221 — 230, First published on: 01 March 2008 (iFirst)

To link to this Article: DOI: 10.1080/10402000801918056

URL: http://dx.doi.org/10.1080/10402000801918056

Tribology Transactions, 51: 221-230, 2008

ISSN: 1040-2004 print / 1547-357X online
DOI: 10.1080/10402000801918056

The Effect of Novel Surface Textures on Tappet Shims on Valvetrain Friction and Wear

ARUP GANGOPADHYAY AND DOUGLAS G. MCWATT
Research and Innovation Center
Ford Motor Company
Dearborn, MI 48121

In an engine, the valvetrain contributes about 6–10% of the total frictional loss depending on the architecture. The cam and the tappet contact in a direct acting mechanical bucket-type valvetrain offers opportunities for friction reduction. Work has been done in the past to reduce the frictional loss at the cam and tappet contact through use of lightweight materials to reduce the reciprocating mass, the improved surface finish, and the low friction thin film coatings. This investigation explored the potential for additional friction reduction through the use of novel surface textures on tappet shims. The surface textures were produced on tappet shims using two techniques: (a) regular patterns like parallel line V-grooves, and square grooves, circular V-grooves, and spiral V-grooves using a diamond tool, and (b) random irregular dimples using either ceramic peening or steel shot peening. The friction performance of these shims was compared with standard production shims and isotropic finish on production shims. Friction was measured using a motored valvetrain rig using a 3.0 L cylinder head. The friction response was different on each type of groove and dependent on the speed and the oil temperature. The shims with parallel line V-grooves showed the highest friction reduction (up to 35%) compared to the production shims. There appears to be no significant difference in wear pattern on cam lobes tested against production shims and shims with parallel line V-grooves. Also, the wear rate of a shim with parallel line V-grooves was no worse than the production shims. The random dimples created by peening did not offer any friction reduction, probably due to the increased surface roughness.

KEY WORDS

Surface Textures; Valvetrain; Friction; Wear; Radionuclide Technique; Engine Oil; Ceramic Peening; Steel Shot Peening

Presented at the STLE/ASME International Joint Tribology Conference in San Antonio, Tx October 23-25, 2006
Manuscript received March 1, 2006
Manuscript approved October 27, 2007
Review led by Alan Lebeck

INTRODUCTION

Customers, manufacturers, and governments are increasingly interested in improved fuel economy of cars and trucks. The corporate average fuel economy (CAFE) for trucks increased in MY 2005 to 21.0 mpg from 20.7 mpg and it will reach 22.2 in MY 2007. Although the CAFE for cars did not increase for the past several years, it is also expected to increase. There are several advanced engine and transmission technologies currently being investigated for improving the fuel economy. The frictional loss in an engine contributes significantly to reduce the fuel economy. The valvetrain contributes about 6–10% of the total frictional loss in an engine, depending on the architecture (Kiovsky, et al. *(1)*). The direct acting mechanical bucket–type design, while offering a lower cost and a lower cylinder cover height, contributes to a higher frictional loss due to the sliding action between the cam lobe and the tappet shim compared to the roller follower design. Therefore, if the frictional loss in a direct acting mechanical bucket (DAMB)-type valvetrain could be brought closer to the roller follower design, it would be possible to gain benefits both from the cost and the fuel economy points of view. This is particularly important because the volume of the engines with DAMB valvetrains is expected to increase in the future. In the direct acting mechanical bucket tappet design, 85–90% of the frictional loss is at the cam and the tappet contact (Comfort *(2)*). There has been a lot of work done in the past to reduce frictional loss at the cam and the tappet contact. The cam and tappet contact in this valvetrain configuration works primarily in the mixed lubrication regime and, therefore, past work focused on reducing friction by using lightweight materials and surface engineering on the tappet surface since it is relatively easy to work with because of its simple geometry. Fukuoka, et al. observed a 40% reduction in the friction torque by reducing the reciprocating mass, i.e., replacing steel tappets with aluminum tappets with thinner walls, and an aluminum spring retainer (Fukuoka, et al. *(3)*). Others tried to reduce friction by reducing the surface roughness at the contact to move the lubrication regime to a more mixed region by increasing the specific lubricant film thickness. Masuda, et al. *(4)* and Katoh and Yasuda *(5)* showed that a significant reduction in valvetrain friction torque can be obtained if the surface roughness of both the camshaft and the inserts are reduced. It has been reported that silicon nitride inserts with mirror-finish surfaces ($R_a - 0.02\ \mu m$) reduced valvetrain friction by about 20–25% in a motored test, which translated into 2–3% improvement in the fuel economy in a Japanese driving cycle (Izumida, et al. *(6)*). The use of silicon nitride inserts appears additionally attractive because of its rigidity, light weight, and higher wear resistance. Gangopadhyay et al. demonstrated that the finishing method applied to achieve a very smooth surface can provide additional friction reduction (Gangopadhyay, et al. *(7)*, *(8)*). It is also possible to reduce friction through the deposition of low-friction coatings. Masuda et al. *(4)* also showed that deposition of a hard and thin TiN coating on a mirror-polished (R_a 0.02 μm) steel reduced cam lobe surface roughness to 0.02 μm R_a in a short time. The low surface roughness of both the contacting surfaces achieved a 40% reduction in friction torque compared to a conventionally finished insert. A diamond-like carbon coating has already been evaluated on steel tappet inserts with encouraging results (Schamel, et al. *(9)*). Rao and Cikanek *(10)* applied a solid film lubricant consisting of molybdenum disulfide, graphite, and boron nitride in a thermoset polymer on a tappet shim surface and observed about 15–20% friction reduction at 100°C oil temperature in a motored valvetrain rig. Additional friction reduction was observed when the camshaft was also coated with the same material. Ahn et al. developed a new supercarburized heat treatment process that reduced the valvetrain friction by 25–30%, resulting in 1–3% vehicle fuel economy benefit (Ahn, et al. *(11)*).

Recently, it has been recognized that fine surface patterns can reduce the sliding friction in addition to the surface finish and coatings. With the improvement of laser technology, it is now possible to laser hone cylinder liners for improved performance. A laser is also used to create dimples on the sliding surface for friction reduction. Ryk, et al. observed a 30–40% friction reduction in the laboratory bench tests when a laser-dimpled piston ring slid against a cylinder liner material (Ryk, et al. *(12)*). Ronen, et al. showed through theoretical analysis that the ratio of the dimple depth to the dimple diameter and the area density of the dimples are the two key factors affecting friction (Ronen, et al. *(13)*). Wakuda, et al. *(14)* also observed a substantial friction reduction when sliding a steel pin (line contact) against a dimpled ceramic disk. The dimples were created either by abrasive jet machining or by laser. Both techniques showed a similar friction reduction and 5–20% dimple density performed best under the test conditions used. Golloch, et al. *(15)* evaluated the friction and the wear reduction potential of laser surface texturing in a fired engine using a floating liner technique. The surface of the cylinder liners was modified near the top dead center region by a laser beam to create discontinuous lines of 3 μm long separated by 2 μm horizontally and vertically. The lines were 40–60 μm wide and 10–25 μm deep. Laser-textured liners showed a significant reduction of friction force early on the power stroke when the combustion pressure is the highest. They also observed reduced wear in a 250-h test. A similar kind of friction reduction was observed in a parallel thrust bearing contact, which could have potential application in a seal-less pump with magnetic drives (Etsion *(16)*, *(17)*). Dumitru, et al. observed an extension of failure time with a laser-textured dimpled surface in laboratory pin-on-disk tests (Dumitru, et al. *(18)*). The majority of investigations have been conducted on dimples created by a laser beam. However, Blatter, et al. *(19)* looked at the effect of laserwriting on a surface where fine lines of 3 μm wide and 2 μm deep separated by 20 μm were created by a laser beam. A laboratory pin-on-disk–type test showed a substantial enhancement of failure time by a laserwritten surface compared to an untextured surface.

The exact mechanism for friction reduction with textures is not well understood, although considerable work is currently in progress to elucidate the mechanism. It is envisioned that there are two main effects. One of them is a hydrodynamic effect: as the fluid flow approaches the dimple, the fluid pressure increases, allowing additional load support capability. This reduces the severity of the metal-metal contact, resulting in lower friction. The other effect is that the liquid trapped in the dimple can be considered as a secondary source of the lubricant, which is drawn into the area surrounding the dimple by the relative movement of surfaces (Wang, et al. *(20)*).

The objective of this investigation was to evaluate the friction reduction potential of surface textures in a direct acting mechanical valvetrain application with special attention to the ability to manufacture the textures relatively easily and less expensively.

EXPERIMENTAL DETAILS

Surface Patterns

In this investigation, textures were created by two different techniques: (a) regular patterns using a diamond tool because it was thought to be less expensive than laser technology, and (b) random pattern by shot peening, which is a proven inexpensive technology in the industry. The patterns were created on tappet shims from a production 3.0 L engine.

Figure 1 shows a schematic diagram of the contact geometry between the cam lobe and the tappet shim. The tappet shim is free to rotate on a groove on top of the tappet. The centerline of the cam lobe is offset from the centerline of the tappet and the tappet shim to facilitate the rotation of both the tappet and the tappet shim, which reduces friction. The shims are made out of AISI 52100 steel having a hardness of 62 R_c and have 0.1–0.2 μm (4–8 μin) centerline average roughness. The camshafts were made out of induction-hardened chilled cast iron having a surface hardness of R_c 50. The camshaft consisted of three sets of camlobes at 120° apart as shown in Fig. 2. Each set consisted of

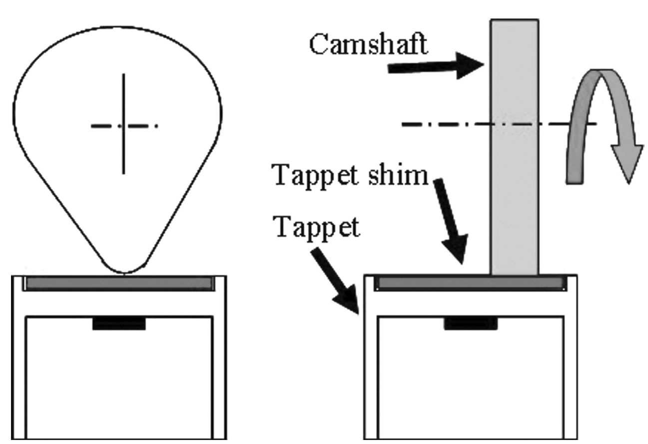

Fig. 1—A schematic diagram of the cam and tappet contact geometry.

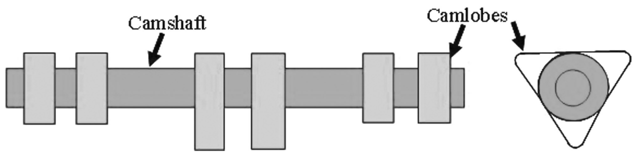

Fig. 2—A schematic drawing showing the position of camlobes on a camshaft.

two camlobes oriented the same way with respect to the camshaft. Figure 3 shows three different types of patterns produced by a diamond tool. They are (a) parallel lines whose cross section could be either V-groove or square groove, (b) concentric circles with V-grooves, and (c) spiral V-grooves. The groove details are shown in Table 1. The width of the contact patch between the cam lobe and the shim is about 80 μm at the nose of the camlobe where the spring force is the highest. The width of the groove was chosen so that the grooves are fully covered by the contact patch to build sufficient hydrodynamic pressure. However, it should be kept in mind that the contact patch size changes with the rotation of the camlobe due to reduced spring force. The production shims have 4–8 μm thick Mn-phosphate break-in coating. It is a soft coating and wears away with time. Textures were prepared on these shims before the coating was deposited because it was anticipated that during evaluation, the coating debris may fill the textures, which may not allow an evaluation of the full potential benefit of textures. Since the grooves were made using a diamond tool, occasionally a pile-up of metal was observed on the side of the grooves and it was removed by light lapping without altering the original surface roughness substantially. A clearance of 0.038 mm (0.0015 inch) was maintained between the base circle of the camlobe and the shim by using shims of various thicknesses.

The random patterns were created by shot peening using either steel shots or ceramic shots. The impact of the shots on the shim surface created small craters as shown in Fig. 4 by the dark spots. The craters were about 4–6 μm deep. Peening with steel shots created a surface with similar features but the crater depth was less, about 2–3 μm deep. The width of the craters was large and it varied between 75 and 325 μm. The ratio of the width to the depth of these craters may not be optimum for the best friction reduction. These craters can act as micro-reservoirs for lubricant. However, a surface profile taken across the shim surface showed that in addition to creating craters, the process also raised metal around the craters. This resulted in a high centerline average roughness of about 1 μm, which is much higher than the production shims.

TABLE 1—THE DETAILS OF GROOVE DESIGN

Grooves	Parallel Line V Grooves	Parallel Line Square Grooves	Circular Grooves	Spiral Grooves
Groove cross section	*V*	Square	V	V
# Of lines/circles	29	29	14	
Groove depth, μm	4	2	4–4.5	2–2.5
Groove width, μm	50	50	50	50
Groove spacing, mm	0.95	0.95	0.95	0.95
Groove volume, mL	0.037	0.037	0.075	0.037
Groove area, %	2.6	2.6	4.98	4.73

Therefore, these shims could show higher friction than the production shims. Attempts were made to remove the raised metal around the craters by lapping on a rotating wheel containing 6 μm diamond paste on a polishing cloth. This step removed the high asperities creating a plateau region while preserving the craters. Figures 5a and 5b compared the surface roughness profile of a ceramic peened shim after peening and peening followed by lapping. This is an attractive process because, if successful, it could be manufactured quite easily and at a reasonable cost.

In addition to various patterns, shims with an isotropic finish were also evaluated for comparison. The isotropic finishing process is a two-step chemo-mechanical process. The first step is called the refining step, where the parts are put into a slowly rotating standard vibratory equipment containing a mild acidic solution and ceramic media. The acidic solution reacts with the metal surface and leaves a very thin soft film, which is then removed by abrasion with the ceramic media. The surface film is continuously reformed and removed resulting in material removal from the surface. The second stage of the process is called the burnishing stage, where a basic solution is added in the vibratory bowl to neutralize the refining solution and also to remove any soft film remaining on the surface. This process results in a very smooth surface, 0.07 μm R_a. This process was selected because it produces the desired finish at a lower cost than other alternatives. The isotropic finishing process was applied prior to the deposition of a break-in coating on tappet inserts.

Friction Measurements

The friction reduction potential of these patterns and structures was evaluated using a motored valvetrain rig as shown in Fig. 6. A cylinder head from a 3.0 L engine was used for the test. The cylinder head was mounted at a 60° angle on an aluminum support

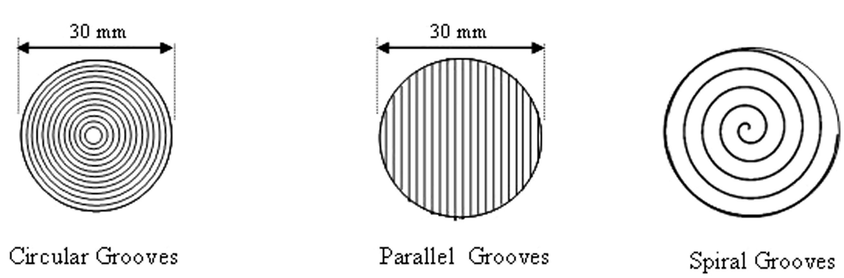

Fig. 3—The design of surface patterns created by diamond tool.

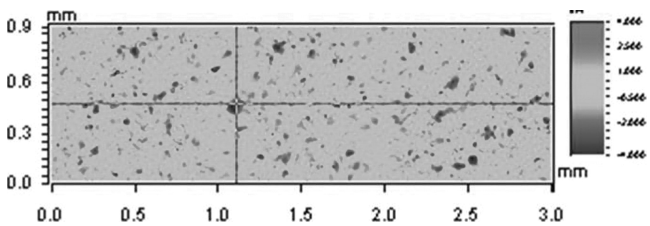

Fig. 4—Shim surface texture following ceramic peening.

to represent the actual orientation in this engine. This engine has four camshafts, two in each bank. Only one camshaft was used for this investigation and it was driven by an electric motor through a flywheel and a set of couplings. An in-line torque meter measured the average torque. Each camshaft contained six camlobes, which slid against six tappet shims. One of the design features of the valvetrain system is that the center of the camlobe was at an offset from the center of the tappet insert to allow the tappet rotation. Therefore, the orientation of grooves with respect to the sliding direction of the camlobe is not an important factor. Factory fill GF-3 SAE 5W-20 oil was used at various temperatures. Engine oil was heated externally in a sump and then pumped into the engine inlet from where it flowed through the original channels to lubricate the cam and tappet contact. The lubricant pressure was maintained at 40 psi. The coolant was also heated in an external sump and then pumped into the engine inlet from where it flowed through the original channels just like engine oil. The circulation of the hot coolant helped to bring the cylinder head to the required temperature quickly.

Prior to the evaluation of each pattern, it was important to ensure that the surfaces of the camlobes and the tappet shims were adequately broken-in. Therefore, for each new set of tappet shims, the camshaft was driven at different speeds from 300 RPM to 2500 RPM at 80°C oil temperature. The speed was changed every 2–3 h while recording the friction torque. Break-in was considered complete when a stable friction torque was observed at each speed. This generally took about 150 h. Separate camshafts were used for the evaluation of each type of the shims to take into account any manufacturing variations that would produce more robust results.

Wear Measurements

The wear of the production shim and the shim with parallel line V-grooves was measured using a laboratory cam/tappet apparatus (Gao, et al. *(21)*) attached with a radionuclide measurement system. The rig essentially consists of a single camlobe from a 2.0 L Zetec production engine, which is driven by a 2 horsepower motor against a direct acting mechanical bucket tappet with a removable insert. This apparatus uses a 27 mm diameter shim, whereas the previous engine uses a 30 mm diameter shim. Therefore, the shim diameter was reduced to 27 mm prior to creating parallel line V-grooves. In the new shim, the depth of the grooves was about 10–12 μm while the width and the spacing remained the same as before. A steel valve having a mass equivalent to a production valve was used with a production valve spring. The tappet reciprocated in an aluminum bore made out of a production cylinder head. The center of the camlobe was at an offset from the center of the tappet shim to allow tappet rotation and reduce the friction torque (Willermet, et al. *(22)*, *(23)*). The camlobe/shim contact area is lubricated by a jet of lubricant at 100°C at 85 psi. The friction torque was also measured by a torque meter mounted in-line with the drive shaft. The top 30 μm surface layer of the uncoated tappet shim was radioactivated to Co^{56} by bombarding the surface with a proton beam. The entire top surface of the shim was activated. The initial radioactivity level on the surface was 5–10 MBq. When the radioactive tappet shim was placed under the rotating camlobe, radioactive wear debris was generated. The debris is carried by the lubricant to a radiation detector where the intensity of gamma rays is measured and then converted into mass loss or wear depth by appropriate computer software. This results in continuous on-line wear monitoring. The engine oil used was GF-4 SAE 5W-20 viscosity grade. The wear measurements were conducted at three different camshaft speeds: 500, 1000, and 1500 RPM to evaluate the effect of speed on wear. At each speed, wear was measured for 2.5 h and then the speed was increased to the next higher level. The total test length was 100 h.

RESULTS AND DISCUSSIONS

In a direct acting mechanical valvetrain, the oil film thickness and thereby the lubrication regimes at the camlobe and tappet

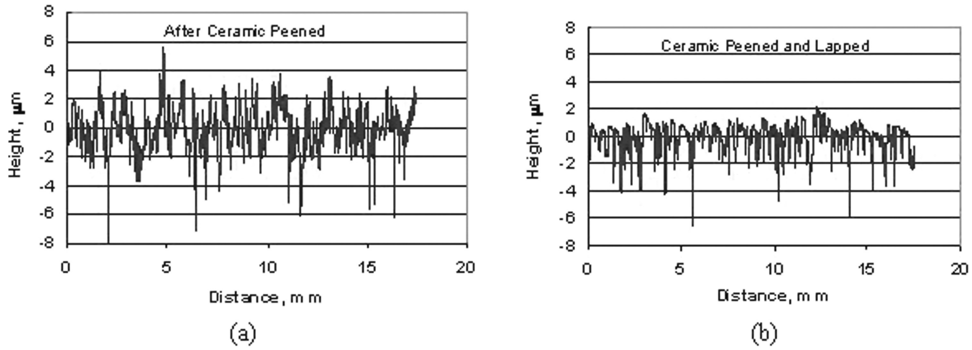

Fig. 5—A typical surface profile of shims (a) after ceramic peening and (b) ceramic peening followed by lapping.

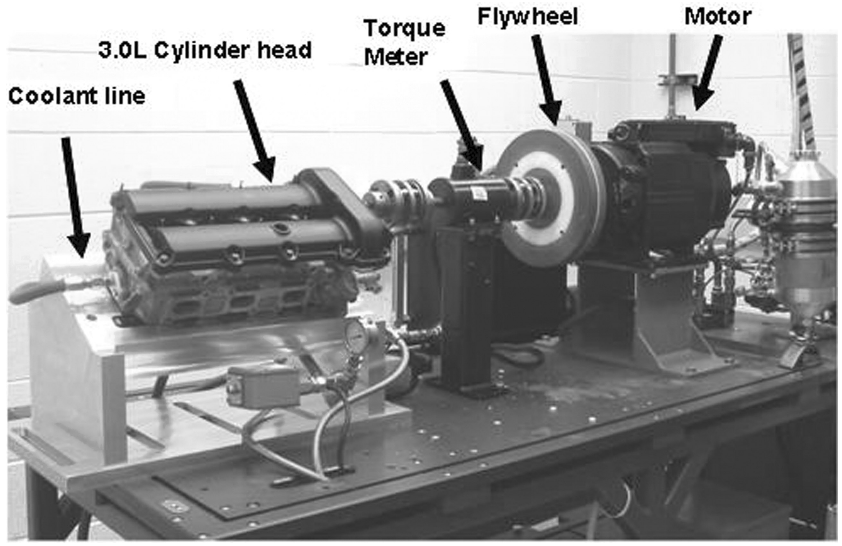

Fig. 6—The motored valvetrain rig for friction measurements.

shim contact varies depending on the camlobe profile during one revolution of the camshaft. At the nose of the camlobe, the contact stress is the highest and the film thickness is the lowest, which renders the contact to operate under the boundary lubrication regime. In the ramp area, the contact stress drops significantly, resulting in a larger oil film thickness and the contact operates in the mixed lubrication regime. The oil film thickness and the lubrication regime also depend on camshaft speed. The friction torque at a given speed is the average friction torque for one rotation of the camlobe, taking into account the oil film thickness and the resulting lubrication regimes.

Friction Performance with Grooved Shims

Figure 7 shows the average friction torque as a function of speed at 100°C oil temperature using a production cam and production tappets and tappet shims. The data clearly demonstrate that the camlobe/tappet shim contact operates primarily in the mixed lubrication regime. Figure 7 also shows excellent repeatability of data. Test 1 and Test 2 were run on two different days under the same test conditions demonstrating how well the system repeats data. The same level of repeatability was observed at other temperatures investigated. The variation of friction torque as a function of camshaft speed is shown in Fig. 8 at different oil temperatures using the production camshaft and the tappet shims. The friction torque decreased as the oil temperature decreased. This is due to increased oil viscosity, resulting in higher oil film thickness and thereby reducing the severity of asperity interactions. Also, with decreased temperature the friction torque variation with the camshaft speed becomes less compared to that at higher temperatures. The higher the temperature, the higher the change in friction torque with speed.

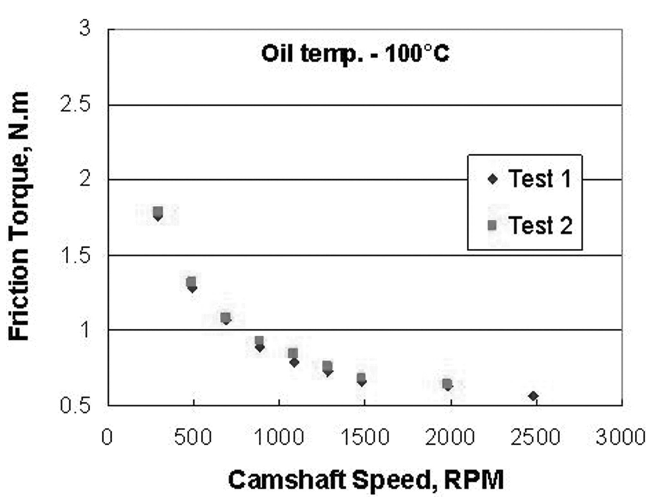

Fig. 7—A typical plot of the variation of valvetrain friction torque with camshaft speeds.

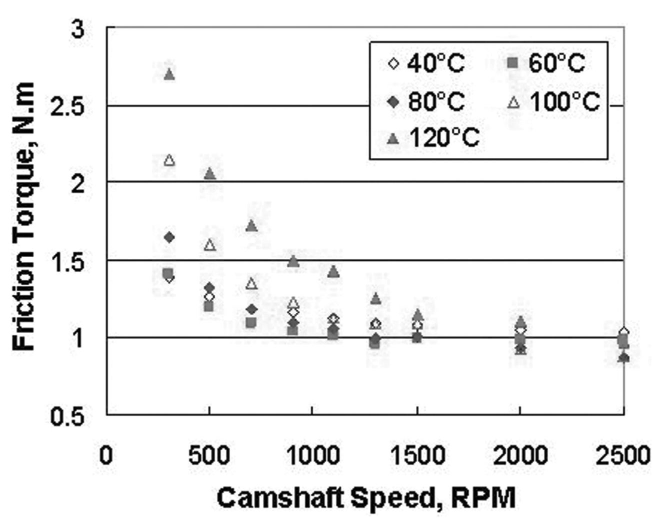

Fig. 8—The valvetrain friction torque as a function of engine oil temperature.

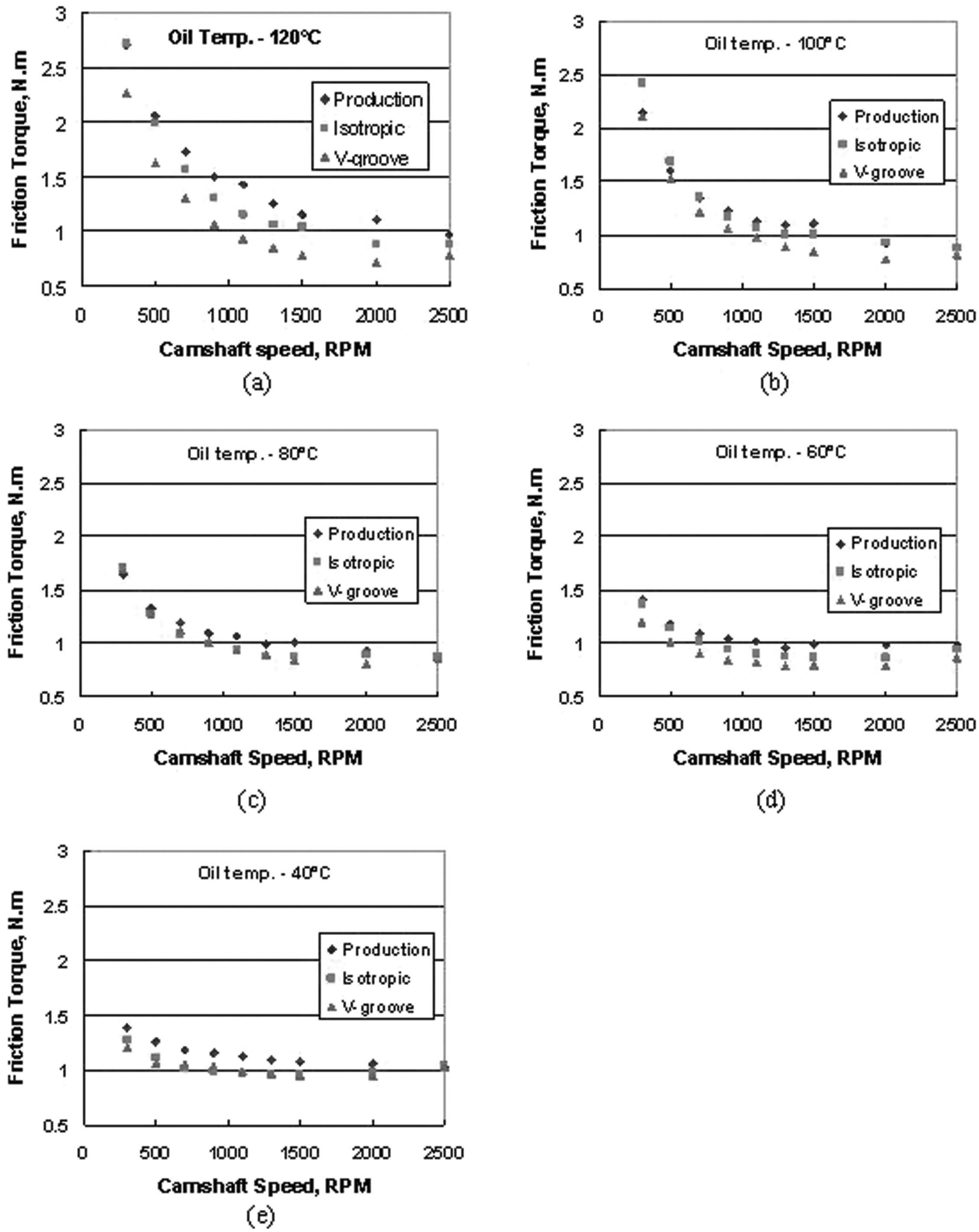

Fig. 9—The friction torque observed with parallel line V-groove and isotropic finish tappet shims and compared those with that of production shims at different temperatures using an exhaust camshaft. (a) 120°C, (b) 100°C, (c) 80°C, (d) 60°C, and (e) 40°C.

Figure 9 compared the friction torques observed with production tappet shims with those of parallel line V-groove shims and isotropic finish shims at different oil temperatures using an exhaust camshaft. The isotropic finish shims showed similar friction torques as observed with the production shims at low camshaft speeds less than 500 RPM but exhibited lower friction torque at higher than 500 RPM. This was observed almost at all oil temperatures but the degree of the friction torque improvement varied with the oil temperature. The parallel line V-grooves showed lower friction torque than the production shims at all speeds and at all temperatures. The friction torques observed with the parallel line V-grooves were also lower than the isotropic finish shims, particularly at higher temperatures when relatively more boundary contact is expected than at lower temperatures where the lubrication regime is less boundary due to increased viscosity. The percentage improvement in the friction torque for the isotropic finish shims and parallel line V-groove shims over the production shims was dependent on the camshaft speed and the oil temperatures.

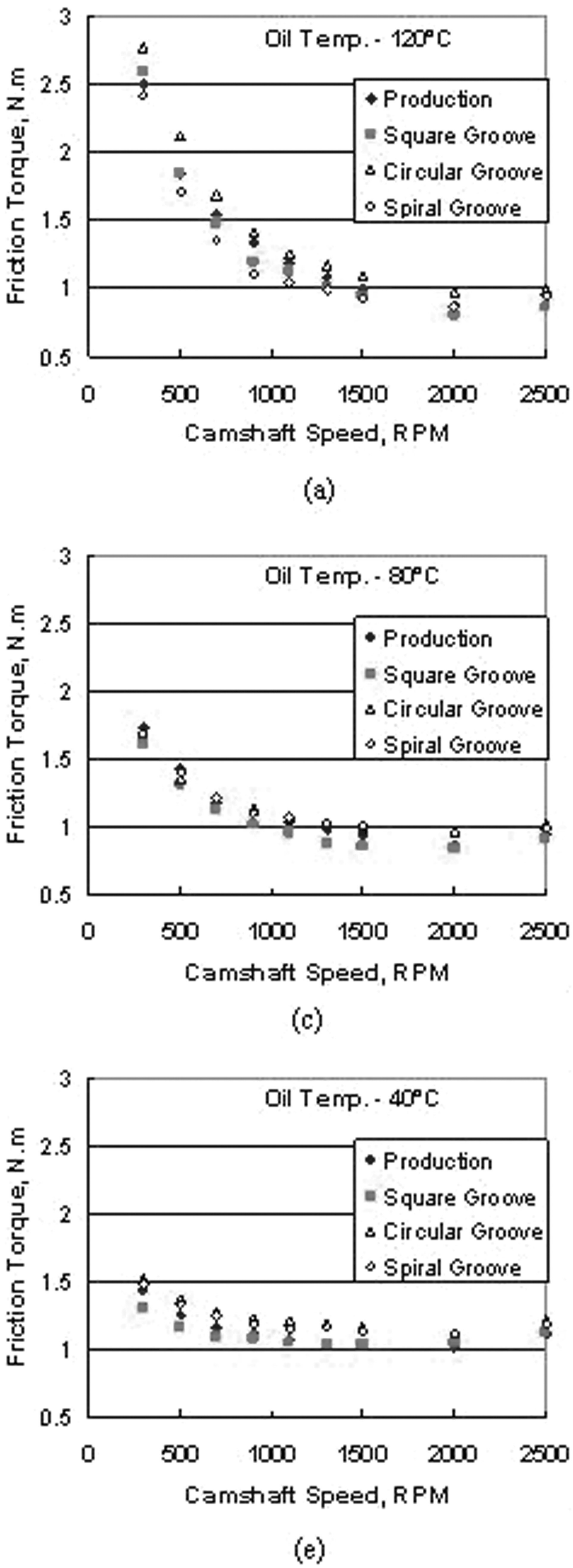

Fig. 10—A comparison of friction torques obtained with parallel square grooves, circular V-grooves, spiral V-grooves and production shims using an intake camshaft at different temperatures. (a) 120°C, (b) 100°C, (c) 80°C, (d) 60°C, and (e) 40°C.

In the case of isotropic finish, an improvement of up to 20% was observed at 120°C in the speed range 300 RPM–1500 RPM. In the case of parallel line V-grooves, the percentage improvement of the friction torque over the production shims also varied between 15 and 35% in the speed range 300 RPM–1100 RPM depending on the oil temperature. It is important to have a large friction reduction at lower camshaft speeds because during fuel economy testing using the FTP (Federal Test Procedure), a significant amount of time is spent at lower engine speeds. In the case of parallel line V-grooves, the minimum friction torque was observed around 2000 RPM, whereas for the production shim, the minimum friction torque was not clearly observed for the speed range investigated and therefore was expected to be at a speed greater than 2500 RPM. Therefore, it can be stated that parallel line V-grooves shifted the Stribeck curve to the left lower corner and at least by 500 RPM.

Figure 10 compared the friction torques observed with the production shims with those observed with parallel line square groove shims, circular V-groove shims, and spiral V-groove shims at different temperatures with an intake camshaft. Since the lift and the profile of the intake and the exhaust camshafts are a little different, the friction torque response is also expected to be slightly different. Therefore, for the sake of fair comparison, experiments were conducted with the production shims also. The friction torques observed with the parallel line square V-groove shims were very similar to the production shims at all camshaft speeds and at all oil temperatures. The circular V-groove shims showed very similar friction torque characteristics as the production shims except at 120°C and 60°C where the friction torque with the circular V-grooves was higher than the production shim. The friction torque observed with the spiral V-groove shims was similar to the production shims except at 120°C, where the friction torque was lower than the production shims. There appears to be no significant difference in the wear pattern on camlobes tested against production shims and the shims with parallel line V-grooves as shown in Fig. 11. Figure 12 shows optical micrographs of the production shims and the parallel line V-groove shims at the end of tests. There are some faint wear marks on all the shims, which are normal, due to shim rotation. No significant difference in the wear patterns was observed on parallel line V-groove shims compared to those of the production shims.

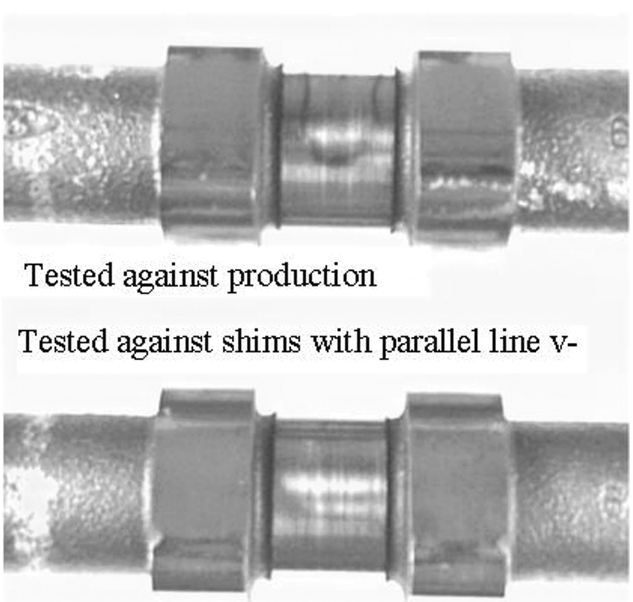

Fig. 11—The appearance of camlobes tested against production shims and shims with parallel line V-grooves.

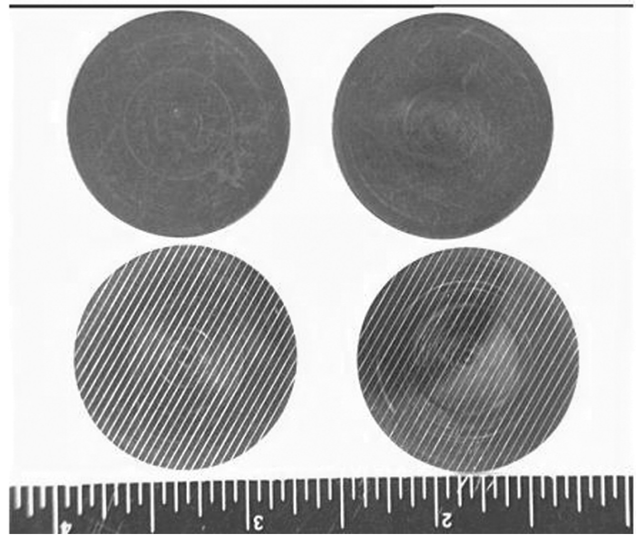

Fig. 12—Optical micrographs of tappet shims at the end of tests; (a) production shims at top row and parallel line V-groove shims at the bottom row.

Wear Characteristics

Figure 13 shows the wear of the production tappet shim without the break-in coating and the parallel line V-groove shim for the 100-h test. The shim with the parallel line V-groove was selected because it showed the highest friction reduction. A separate

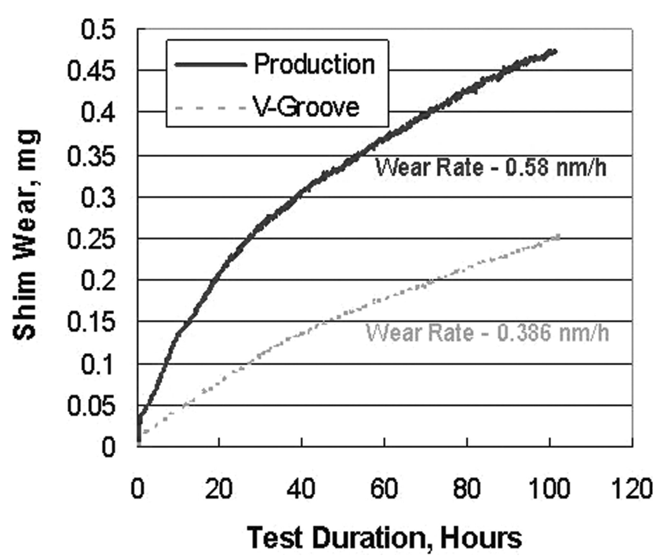

Fig. 13—A comparison of wear characteristics of production and parallel line V-groove tappet shims.

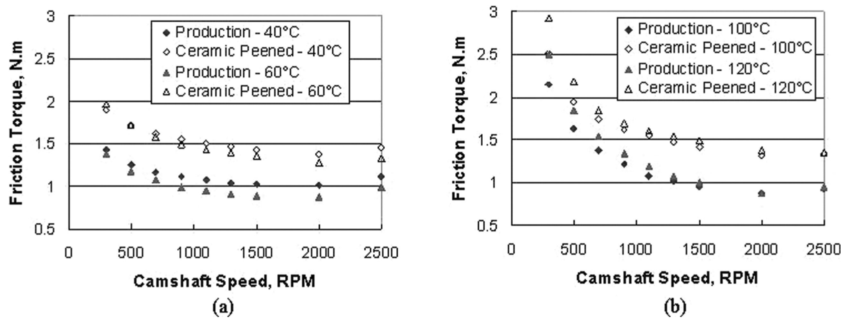

Fig. 14—A comparison of the friction torque observed with the ceramic peened shims and production shims at (a) 40°C, and 60°C, and (b) 100°C, and 120°C oil temperatures.

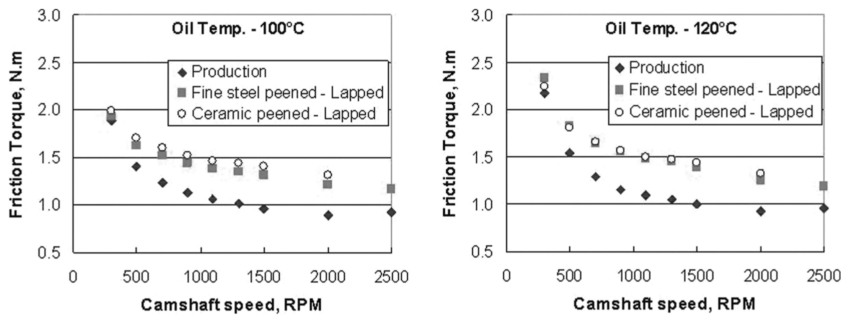

Fig. 15—A comparison of the friction torque observed with fine steel peened, and ceramic peened shims followed by lapping and production shims at (a) 100°C and (b) 120°C oil temperature.

camlobe was used for each shim. The test was conducted for 100 h because it has been observed before (Gangopadhyay, et al. *(24)*) that the wear rate of the shim changes very rapidly for the first 50 h of the test due to the break-in of the surfaces, after which the wear rate changes only a little. Therefore, a 100-h test was considered optimum to compare the wear performance. The total wear observed with the parallel line V-groove shim was much less than the production shim. The initial high wear rate of the production shim could be related to the higher surface roughness of the camlobe used against it. The centerline average surface roughness of the camlobe used against the production shim and the V-groove shim was 0.56 μm and 0.28 μm R_a, respectively. Although the R_a values may appear to be significantly different, it is within the manufacturing specification. The wear rate is a better parameter to compare the wear performance for the long-term performance characteristics. The wear rate of the tappet shim with parallel line V-grooves was lower than the production shim. Although it may be possible that some wear debris may be lodged in the grooves and may not be carried away by the lubricant (Varenberg, et al. *(25)*), it can be said that the wear rate of the V-groove shims are no worse than the production shims, if not better. The wear rate was calculated for the 50-100 hour test duration following the break-in. The small wear rate of the shim with the parallel line V-groove indicates that the effect of the grooves on friction will likely be preserved for the life of the engine, although additional tests are required for verification.

Based on these results it is clear that both the isotropic finish and the parallel line V-grooves demonstrated a reduction in the friction torque at all oil temperatures and out of these the parallel line V-grooves showed the most friction reduction. The shims with parallel line V-grooves also demonstrated a lower wear rate than the production shim.

Figure 14 compared the friction torques observed with the ceramic peened tappet shims and the production shims. A different exhaust camshaft was used for these experiments. The centerline average roughness of the ceramic peened shims was 1.2 μm. The graphs show that the ceramic peened shims did not show any improvement in the friction torque over the production shims at 40°C, 60°C, 100°C, and 120°C oil temperatures. On the contrary, higher friction torques were observed. This could be due to the higher roughness on the shims created by peening. Figure 15 compared the friction torques observed with fine steel shot peened and ceramic peened shims followed by lapping with the production shims. The centerline average roughness of fine steel peened shims before and after lapping were 0.6 μm and 0.4 μm, respectively, and for ceramic peened shims after lapping was 0.8 μm. Although lapping removed high asperities on the surface, the size of valleys to retain oil was probably not large enough to create a high lubricant pressure to reduce the friction.

CONCLUSIONS

Based on the present investigation, it can be concluded that

- the presence of a novel fine surface texture on a tappet shim can reduce the friction but not all the surface textures are effective friction reducers.
- parallel line V-grooves reduced friction the most.

– shims with an isotropic finish also reduced friction but not to the same extent as the parallel V-grooves.
– the extent of friction reduction was dependent upon the speed and the oil temperature.
– the creation of a random texture by peening (either by ceramic or steel shot) produced a higher surface roughness, resulting in higher friction than the production shim. Removal of high asperities created by peening by subsequent lapping did not show any friction improvement over the production shims.
– the wear rate of the parallel line V-grooves shim was no worse than the production shims. The wear pattern on camlobes tested against parallel line V-groove shims was similar to that tested against the production shims.

ACKNOWLEDGEMENTS

The authors would like to acknowledge the assistance of Bob Cross, Dennis Roper, Greg Ciavattone, and Nick Wade in the Ford RIC Components Laboratory for the design, installation, troubleshooting, instrumentation, and setting up the data acquisition system, Sherry Lopez for generating the CAD drawing of parts, the machine shop personnel for the fabrication of parts, and Cory Phillips for acquiring wear data using the radionuclide measurement system.

REFERENCES

(1) Kiovsky, T. E., Yates, N. C. and Bales, J. R. (1994), "Fuel Efficient Lubricants and the Effect of Special Base Oils," *Lub. Engg.*, **50** (4), p 307.
(2) Comfort, A. (2003), "An Introduction to Heavy-duty Diesel Engine Frictional Losses and Lubricant Properties Affecting Fuel Economy—Part I," SAE 2003-01-3225.
(3) Fukuoka, S., Hara, N., Mori, A. and Ohtsubo, K. (1997), "Friction Loss Reduction by New Lighter Valvetrain System," *JASE Review*, **18**, p 107.
(4) Masuda, M., Ujino, M., Shimoda, K., Nishida, K., Marumoto, I. and Moriyama, Y. (1997), "Development of Titanium Nitride Coated Shim for a Direct Acting OHC Engine," SAE paper No. 970002.
(5) Katoh, A. and Yasuda, Y. (1994), "An Analysis of Friction Reduction Techniques for the Direct Acting Valvetrain System of a new Generation Lightweight 3-Liter V6 Nissan Engine," SAE paper No. 940992.
(6) Izumida, H., Nishioka, T., Yamakawa, A. and Yamagiwa, M. (1997), "A Study of the Effects of Ceramic Valvetrain Parts on Reduction of Engine Friction," SAE paper No. 970003.
(7) Gangopadhyay, A. K., McWatt, D., Willermet, P. A., Crosbie, G. M. and Allor, R. L. (1999), "Effects of Composition and Surface Finish of Silicon Nitride Tappet Inserts on Valvetrain Friction," in *Proc. of the 25th Leeds-Lyon Symposium on Tribology*, Tribology Series 36, Lyon, Sept. 8-11, pp 635-644.
(8) Gangopadhyay, A. K., Soltis, E. and Johnson, M. D. (2004), "Valvetrain Friction and Wear: Influence of Surface Engineering and Lubricants," in *Proc. Instn. Mech Engrs.* **218**, Part J, pp 147-156 (*J. Engineering Tribology*).
(9) Schamel, A. R., Grischke, M. and Bethke, R. (1997), "Amorphous Carbon Coatings for Low Friction and Wear in Bucket Tappet Valvetrains," SAE paper No. 970004.
(10) Rao, V. D. N. and Cikanek, H. A. (1994), "1.8L Sierra-Mondeo Turbo Diesel Valvetrain Friction Reduction Using Solid Film Lubricant," SAE paper No. 941986.
(11) Ahn, S. G., Ban, H. O., Jo, B. L., Kim, S. C. and Jung, S. C. (2000), "Development of Supercarburized Tappet Shim to Improve Fuel Economy," SAE paper No. 2000-01-0613.
(12) Ryk, G., Kligerman, Y. and Etsion, I. (2002), "Experimental Investigation of Laser Surface Texturing for Reciprocating Automotive Components," *Trib. Trans.*, **45**, pp 444.
(13) Ronen, A., Etsion, I. and Kligerman, Y. (2001), "Friction Reducing Surface Texturing in Reciprocating Automotive Components," *Trib. Trans.*, **44**, 3, pp 359.
(14) Wakuda, M., Yamauchi, Y., Kanzaki, S. and Yasuda, Y. (2003), "Effect of Surface Texturing on Friction Reduction Between Ceramic and Steel Materials Under Lubricated Sliding Contact," *Wear*, **254**, pp 356.
(15) Golloch, R., Merker, G. P., Kessen, U. and Brinkmann, S. (2004), "Benefits of Laser Structured Cylinder Liners for Internal Combustion Engines," 14th International Colloquium Tribology, Jan 13-15, 2004, "Tribology and Lubrication Engineering," Eds Wilfred Bartz, Vol 1.
(16) Etsion, I. (2005), "State of the Art in Laser Texturing," *J. Tribology*, **127**, pp 248-253.
(17) Etsion, I. (2004), "Laser Surface Texturing—Measure to Reduce Friction", 14th International Colloquium Tribology, Jan 13-15, "Tribology and Lubrication Engineering," Ed. Wilfred Bartz, Vol 1, p 329.
(18) Dumitru, G., Romano, V., Weber, H. P., Haefke, H., Gerbig, Y. and Pfluger, E. (2000), "Laser Microstructuring of Steel Surfaces for Tribological Applications," *Appl. Phys.*, **A70**, pp 485.
(19) Blatter, A., Maillat, M., Pimenov, S. M., Shafeev, G. A. and Simakin, A. V. (1998), "Lubricated Friction of Laser Micro-Patterned Sapphire Flats," *Trib. Lett.*, **4**, p 237.
(20) Wang, X., Kato, K., Adachi, K. and Aizawa, K. (2003), "Loads Carrying Capacity Map for the Surface Texture Design of SiC Thrust Bearing Sliding in Water," *Trib. Inter.*, **36**, p 189.
(21) Gao, H., Gangopadhyay, A. K., McQueen, J. S., Black, E. D., Jensen, R. K., Bjornen, K. K. and Soltis, E. A. (2003), "Antiwear Performance of Low Phosphorous Engine Oils on Tappet Insert in Motored Sliding Valvetrain Test," SAE paper No. 2003-01-3119.
(22) Willermet, P. A. and Pieprzak, J. M. (1989), "Some Effects of Lubricant Composition and Tappet Rotation on Cam/Tappet Friction," *J. of Tribology*, **111**, p 683.
(23) Willermet, P. A., Pieprzak, J. M. and Dailey, D. P. (1990), "Tappet Rotation and Friction Reduction in a Center Pivot Rocker Arm Contact," *J. of Tribology*, **112**, p 655.
(24) Gangopadhyay, A. K., Carter III, R. O., Simko, S., Gao, H., Bjornen, K. K. and Black, E. D. (2007), "Valvetrain Friction and Wear Performance with Fresh and Used Low Phosphorous Engine Oils," *Trib. Trans.*, **50**, 3, pp 350-360.
(25) Varenberg, M., Halperin, G. and Etsion, I. (2002), "Different Aspects of the Role of Wear Debris in Fretting Wear," *Wear*, **252**, pp 902-910.